Calculation of the first two ionization potentials of einsteinium and holmium using relativistic coupled cluster method

J. M. de Wit
Supervisors: A. Borschevsky and R.W.A. Havenith

June 2016

The calculation of the first and second ionization potentials (IPs) of einsteinium and holmium are presented. They are performed in the framework of the Dirac-Coulomb Hamiltonian. Electron correlation is treated using the relativistic coupled cluster method, including single, double and perturbative triple excitations (CCSD(T)). Comparisons are made with experimental results for the first IPs and with theoretical values obtained in earlier research for the second IPs. Also non-relativistic results are presented. Calculations are done on elements of group 1 of the periodic table (lithium till ununennium) and group 12 (zinc till copernicium), varying the method (relativistic Dirac-Hartree-Fock (DHF) and relativistic coupled cluster), the basis sets (double-zeta, triple-zeta and quadruple-zeta) and the approach (four-component, two-component and non-relativistic) used. In this way, the best combination of variables could be obtained for performing the calculations on einsteinium and holmium.

1 Introduction

Uranium (Z=92) is the heaviest atom found in nature. Atoms heavier than uranium do not occur naturally, but are man-made. These elements are called transuranium elements (figure 1) and they are fascinating objects for scientists to study. These transuranium elements are all nuclear unstable, because of the large number of protons in their nucleus. Generally, the higher the atomic number gets, the smaller the lifetime of the atom. When the atomic number exceeds 103, we call them super-heavy elements.

Chemical properties of transuranium elements are meaningful to know in order to get a better understanding of the periodic table. Analogies between these elements and their lighter homologues (the lighter elements in the same column) can be found, confirming the positions of the elements in the periodic table. Also the influence of relativity on atomic and chemical properties can be observed. Because the production rate and lifetime of transuranium elements are often very small, experimental research can be very difficult and expensive. Because of this difficulty (or impossibility) of determining their properties experimentally, theoretical research on these elements is very important. In some cases it gives the only useful information about transuranium elements. This information can in turn help in future experimental research.

Elements running from actinium (Z=89) until lawrencium (Z=103) are known as the actinides. These fall into the so called 'f-block', where the 'f' refers to the shell being filled. One of the actinides is einsteinium (Z=99). It was discovered in the fallout of the first hydrogen bomb test in 1952. The discovery of this element was first being kept a secret by the U.S. military, because of the Cold War

and the competition with the Soviet Union in nuclear technologies. The discovery was published in 1955, and it brought new light to scientific research of how elements are formed in the Universe. [1]

Einsteinium now is being produced in nuclear reactors, with a total production value of around one milligram per year. It is the element with the highest atomic number ever observed in macroscopic quantities in pure form. It is a silvery metal, which continuously glows because of its radioactivity. The halflife of its most common isotope (Es-253) is 20,47 days and it is a decay product of californium (Cf-253).

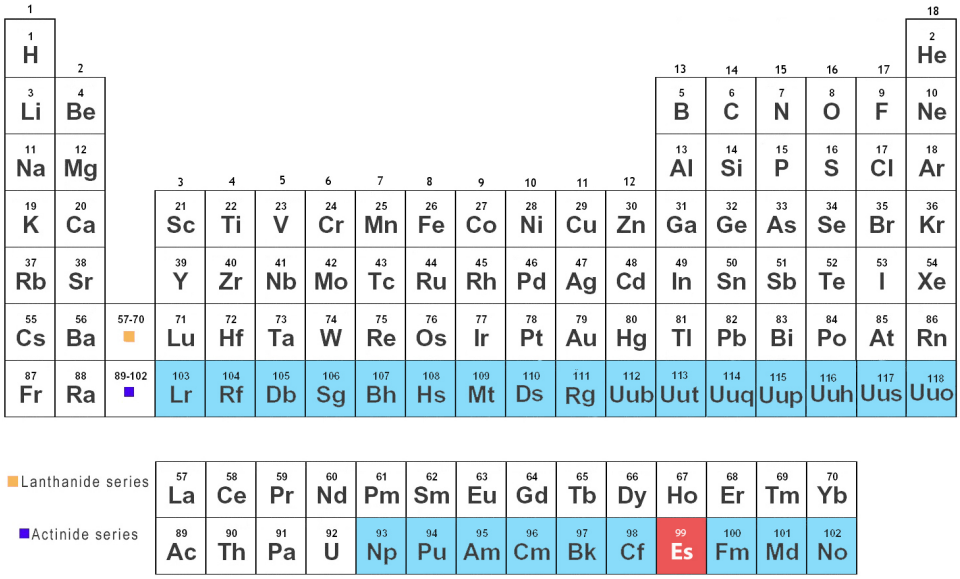

Figure 1: The periodic table with the transuranium elements in blue and einsteinium in red.

Because of self-irradiation, solid einsteinium is self-destructive, destroying its own crystal lattice. This, together with the scarcity and relative short lifetime makes it very difficult for scientists to experimentally determine chemical properties of the element. [2]

One interesting chemical property of an element is the ionization potential. It is the amount of energy you have to put in an atom, in order to remove the valence electron. The ionization potential is an important property to know, since it gives insight about the electronic structure and the chemical behaviour of the atom. In this thesis the results of the theoretical calculation on the first and second ionization potentials of einsteinium and its lighter homologue holmium are presented, using the relativistic CCSD(T) method. These results are compared with experimental values (if available) and other theoretical calculations that were done before.

Furthermore, calculations are carried out on elements of group 12 and group 1 of the periodic table. Different methods are used, in order to determine the best combination of variables to get the most accurate results. Also the difference between relativistic and non-relativistic calculations is presented, to gain insight into the influence of relativity on atomic properties.

2 Method

An atom is a many-body system. It consists of a nucleus and electrons, which are interacting with each other. To determine the ionization potential, we need to know the difference in energy between the neutral atom and the ionized atom. One needs to start with the time-independent Schrödinger equation:

$$E|\Psi\rangle = \hat{H}|\Psi\rangle \tag{1}$$

When it is solved, it will give us the wavefunction $|\Psi\rangle$ and energy E of the system. There are a couple of aspects that need to be considered in order to get accurate results: electron correlation, relativity and basis sets. We will discuss these one by one in this section.

2.1 Electron correlation

One way to deal with solving the Schrödinger equation is by using the Hartree-Fock (HF) method [3]. The theory behind this method is that each of the electrons in the atom can be described by single-particle wavefunctions χ (called orbitals), which are independent of each other. In this approximation, the electron are subjected to an average potential arising from the other electrons, but explicit interactions between the electrons are neglected.

We already know how to solve the Schrödinger equation for the simplest case, the hydrogen atom with only one electron. If we would add another electron to this system, we need to reformulate the wavefunction in our Schrödinger equation. For not interacting particles, we can just take the product of the two orbitals:

$$\Psi(\mathbf{x_1}, \mathbf{x_2}) = \chi_1(\mathbf{x_1})\chi_2(\mathbf{x_2}) \tag{2}$$

Where $\mathbf{x_1}$ and $\mathbf{x_2}$ are the four vectors describing the spatial and spin state of the two orbitals. Since we are dealing with fermions, we need to make sure that our wavefunction obeys the Pauli exclusion principle: we cannot have two fermions in the same state. Therefore, the product in (2) is not sufficient. Lets take a look at the following wavefunction:

$$\Psi(\mathbf{x_1}, \mathbf{x_2}) = \frac{1}{\sqrt{2}}[\chi_1(\mathbf{x_1})\chi_2(\mathbf{x_2}) - \chi_1(\mathbf{x_2})\chi_2(\mathbf{x_1})] \tag{3}$$

Now, if we put the two electrons in the same state, the total wavefunction becomes zero, which is a desirable characteristic of the wavefunction if we want it to obey Pauli's exclusion principle. When we have to deal with more than two electrons, it becomes convenient to work with determinants. For the general case of n electrons, we have:

$$\Psi(\mathbf{x_1}...\mathbf{x_n}) = \frac{1}{\sqrt{n!}}\begin{vmatrix} \chi_1(\mathbf{x_1}) & \chi_2(\mathbf{x_1}) & \dots & \chi_n(\mathbf{x_1}) \\ \chi_1(\mathbf{x_2}) & \chi_2(\mathbf{x_2}) & \dots & \chi_n(\mathbf{x_2}) \\ \vdots & \vdots & \ddots & \vdots \\ \chi_1(\mathbf{x_n}) & \chi_2(\mathbf{x_n}) & \dots & \chi_n(\mathbf{x_n}) \end{vmatrix} \tag{4}$$

which is called the Slater determinant. Using this wavefunction, the calculated energy will always be an upper bound. So to get the best possible value, we need to minimize the energy. We need to start with a choice of orbitals, and iterative vary them until we reach the minimized energy. This is the

basis concept of the Hartree-Fock method.

Even though this method is a good starting point, the fact that the electrons in reality do interact make the results only a crude estimation. To get better results, we need to include electron correlation to account for the explicit interactions between the electrons. There are different ways to do this, and we have used the coupled cluster method [4].

Imagine all the electrons of an atom filling the lowest energy levels, as in figure 2a. These orbitals together are called the filled Fermi sea, which is described by the wavefunction $|\Phi\rangle$. In the Hartree-Fock method, these electrons move independently. When we include interactions, one thing that can happen is that two electrons lift themselves out of the Fermi sea, as in figure 2b. These electrons are correlated and we can describe this process by an operator that is acting on the wavefunction: $S_2|\Phi\rangle$. Here, the two stands for double excitation. This can also happen with two correlated pairs independently, as in 2c. Now the operator S_2 is applied twice: $\frac{1}{2}S_2^2|\Phi\rangle$, where we have to multiply by $\frac{1}{2}$ so the pairs aren't counted twice. The general form of m independent double excitations is then: $\frac{1}{m!}S_2^m|\Phi\rangle$. But m can be any arbitrary number, so to get the total contribution we have to sum over this term and we recognize this sum as the series expansion of e^x:

$$\sum_{m=0}^{\infty} \frac{1}{m!} S_2^m |\Phi\rangle = e^{S_2}|\Phi\rangle \tag{5}$$

As in figure 2d, we see that the same thing can happen with 3 electrons at once. This is called triple excitation and we can treat it in the same way as we did with double excitations. So for n independent triple excitations, we get an contribution of in the form of: $\frac{1}{n!}S_3^n|\Phi\rangle$. A double excitation and a triple excitation can also happen simultaneously. Therefore we get the term $\frac{1}{m!n!}S_2^m S_3^n|\Phi\rangle$. When summed over n and m, we again get an e-power: $e^{S_2+S_3}|\Phi\rangle$. So for all possible types of excitations, we can write the wavefunction as:

$$|\Psi\rangle = e^{S_2+S_3+S_4+\ldots+S_N}|\Phi\rangle = e^{\mathbf{S}}|\Phi\rangle \tag{6}$$

Where N is the total amount of electrons present in the atom and $\mathbf{S}$ represents the sum. The Schrödinger equation can then be written as:

$$E|\Phi\rangle = e^{-\mathbf{S}}\hat{H}e^{\mathbf{S}}|\Phi\rangle \tag{7}$$

This equation yields a set of coupled equations, which can be solved to obtain the energy and the wavefunction of the system.

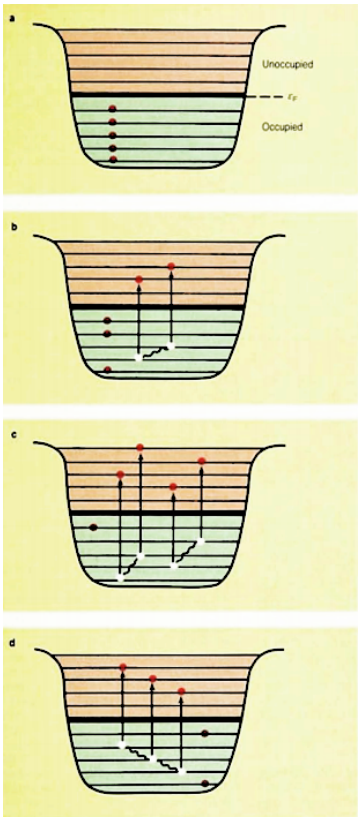

Figure 2: Fermi sea [4]

2.2 Relativity

A larger atomic number means a larger attractive force felt by the electrons. This causes the electrons to move faster. The mass of an electron can be determined by the following formula:

$$m = \frac{m_0}{\sqrt{1 - (\frac{v}{c})^2}} \tag{8}$$

With m_0, v and c respectively being the rest mass of the electron, the velocity of the electron and the speed of light. When the velocity is small compared to the speed of light, the mass of the electron is approximately equal to the rest mass and relativistic effects can be neglected. This is the case for light elements such as lithium. However, when we move up in atomic number, the electrons velocity reaches values for which the mass of the electron increases significantly relative to its rest mass and relativity can't be neglected anymore.

There are three important relativistic effects to consider. First, the radial contraction and energy stabilization of the inner s- and p$\frac{1}{2}$-shells, which are close to the nucleus. This can be explained by looking at the formulas for the radial distance (r) and energy (E) of the Bohr model:

$$r = \frac{Ze^2}{mv^2} \tag{9}$$

$$E = -\frac{2\pi^2 e^4}{n^2 h^2} m Z^2 \tag{10}$$

With e, n and h being the elementary charge, principal quantum number and Planck's constant, respectively. We see that with increasing mass, the radial distance and the energy decreases, leading to a contracted orbital and a stronger bound (more stable) electron. The higher s- and p$\frac{1}{2}$-shells also contract and stabilize, because their spatial distribution is influenced by the inner orbitals (they are orthogonal, which means they can't overlap).

Second, the radial expansion and energy destabilization of the d- and f-shells, which are shielded from the nucleus by the s- and p-shells. The contraction of the inner s- and p-shells causes a better screening from the nuclear charge. As a result, the d- and f-shells are expanded and are energetically destabilized.

Third, the electrons with orbital angular momentum larger than zero experience the spin-orbit splitting, which is an interaction between the electron's motion and spin. This splitting increases with increasing atomic number. It causes a shift in the energy of the orbitals. [5, 6]

So, when doing calculations on heavier elements, one needs to take relativity into account in order to get accurate results. Instead of solving the non-relativistic Schrödinger equation, we will solve the relativistic Dirac equation. This involves the four-component Dirac-Coulomb Hamiltonian:

$$H_{DC} = \sum_i h_D(i) + \sum_{i<j} \frac{1}{r_{ij}} \tag{11}$$

Where h_D is the Dirac Hamiltonian:

$$h_D = c\boldsymbol{\alpha} \cdot \mathbf{p} + \beta c^2 + V_{nuc} \tag{12}$$

Here, $\boldsymbol{\alpha}$ and β are the four-component Dirac matrices, V_{nuc} is the nuclear potential and $\mathbf{p}$ is the four-momentum of the electron.

The wavefunction in the Dirac equation can be written as a four-component vector:

$$\Psi_{4c} = \begin{pmatrix} \Psi^L \\ \Psi^S \end{pmatrix} \tag{13}$$

Where Ψ^L and Ψ^S are both two-component wavefunctions, which correspond to positive energy E^+ (electronic) states and negative energy E^- (positronic) states, respectively. In the four-component relativistic Dirac-Hartree-Fock method, this wavefunction is used to solve the equations. From these results, the negative energy spectrum is then discarded before they are used further in the coupled cluster calculations. This is because we are neglecting positron-electron pair creation.

The two-component wavefunctions can be coupled by the following relation:

$$\begin{aligned} \Psi^S &= R\Psi^L \\ R &= \frac{c(\sigma \cdot \mathbf{p})}{2mc^2 - V_{nuc} + E^+} \end{aligned} \tag{14}$$

Where σ represents the Pauli spin matrices. This coupling term R can be used to express the four-component wavefunction Ψ_{4c} only in terms of Ψ^L, resulting (after several manipulations) in a two-component wavefunction:

$$\Psi^+_{2c} = \sqrt{1 + R^\dagger R}\Psi^L \tag{15}$$

Where $R^\dagger$ is the hermitian conjugate of R. Using R, we can also define a two-component Hamiltonian. It reproduces the positive-energy spectrum of the four-component Hamiltonian h_D. Using this Hamiltonian instead of the one given in (12) is known as the two-component approach. In general it will give less accurate results, because some information is lost due to the fact that we are leaving out Ψ^S. However, two-component approaches can reproduce the full relativistic results very well. Since it also requires less computational resources and has a significantly smaller run time, two-component approaches are a very good alternative to four-component approaches. [7, 8]

2.3 Basis set

The single-particle wavefunctions or orbitals χ are mathematically described by linear combinations of basis functions. This set of basis functions is called the basis set. The basis functions are again composed of linear combinations of Gaussian functions and they have the following form:

$$g_{ijk} = Nx^i y^j z^k e^{-\alpha r^2} \tag{16}$$

Where i, j and k are non-negative integers, N is a normalization constant and α is a positive orbital exponent.

The smallest (or minimal) basis set is the one which only uses one basis function per orbital. This set can be expanded to create a larger set, which increases the accuracy of the results. This can be done by adding more basis function per valence orbital (split valence basis sets). To indicate how many

basis functions per valence electron a basis set has, we call them double-zeta (two basis functions), triple-zeta (three basis functions), quadruple-zeta (four basis functions), and so on.

Even more accuracy can be realized when orbitals with different shapes are added (polarized basis sets). For example, the minimal set of a hydrogen atom only has a basis function which describes the only orbital present, the s-orbital. In a polarized basis set, there would also be a basis function describing a p-orbital. This gives more accurate results.

Another way to improve the basis set is to add diffused functions. These functions occupy a larger amount of space, and can be important when we are dealing with electrons that are far away from the nucleus. [9]

2.4 Overview of method used

The calculations were carried out using the DIRAC15 program [10] in the framework of the four-component Dirac-Coulomb Hamiltonian. For the two-component approach we have used one of the most accurate Hamiltonians, the exact two-component relativistic Hamiltonian (X2C) [8]. We produced the non-relativistic results by setting the speed of light in the input to a very large number (compared to 137,036 Hartree, which is the speed of light in atomic units), such as 10000 Hartree. In this way, the lower part of the wavefunction in (13) vanishes and the upper part will term into the non-relativistic solutions [11]. We have used the double-zeta, triple-zeta and quadruple-zeta Dyall valence basis sets [12]. These relativistic sets were developed with the Dirac-Coulomb Hamiltonian and a Gaussian nuclear charge distribution.

3 Results and discussion

3.1 Examining different methods and the influence of relativity

In order to get a feeling about the different methods, different basis sets and the influence of relativity, we started with some calculations on elements of group 12 and 1, from which most of the IPs are experimentally known. In section 3.1 we start with comparing first IPs of group 12 elements obtained with different methods and different basis sets. In this way, we can make conclusions about which method and basis set is best. For the elements of group 1, we calculate the relativistic and non-relativistic first and second IPs within one method. This will give insight about the effects of relativity. In section 3.2 the results of the first and second IPs of einsteinium and holmium are presented.

3.1.1 Ionization potentials of group 12 elements

Comparing DHF, CCSD and CCSD(T)

In table 1 the first IPs of zinc (Zn), cadmium (Cd), mercury (Hg) and copernicium (Cn) are shown, obtained using the relativistic Dirac-Hartree-Fock approach, the relativistic coupled cluster approach with single and double excitations (CCSD) and including perturbative triple excitations, all in the four-component approach. This was done with the triple-zeta Dyall basis set (dyall.v3z). Also the experimental values are shown (cursive). For Cn there is no experimental value available yet. Therefore we compare it to two other theoretical values. One obtained using the relativistic CCSD method

combined with the Dirac-Coulomb-Breit Hamiltonian and universal basis set of Malli [13]. One obtained using the multi-reference configuration interaction method combined with the Dirac-Coulomb Hamiltonian and Dyall quadruple-zeta basis set (dyall.v4z) [14]. We can see that for the elements with accurate known experimental values, the CCSD(T) gives the smallest error, and thus is most accurate.

Table 1: First IPs in eV and their errors with respect to the the experimental value in percents, within the 4c approach and using basis set dyall.v3z, comparing different methods.

	DHF	**Error**	**CCSD**	**Error**	**CCSD(T)**	**Error**	***Experiment***
Zn	7,792	17,0	9,204	2,0	9,369	0,3	*9,394* [15]
Cd	7,355	18,2	8,807	2,1	9,007	0,1	*8,994* [15]
Hg	8,552	18,1	10,214	2,1	10,405	0,3	*10,438* [15]
Cn	11,649(d)	-	11,664(d)	-	11,811(d)	-	11,969 [13]
	11,649(s)		13,324(s)		13,556(s)		11,779 [14]

In general the electronic configuration of the neutral elements of group 12 ends with a closed d-shell and a closed s-shell. For example, for Hg the configuration is $[Xe]4f^{14}5d^{10}6s^2$ [15] and for Cn it is $[Rn]5f^{14}6d^{10}7s^2$ [13]. When the atom is ionized, an electron is removed from the s-shell, so the electronic configuration of the ionized atom Hg^+ looks like $[Xe]4f^{14}5d^{10}6s$ [15], and for Cn^+ it should look like $[Rn]5f^{14}6d^{10}7s$. However, we know that due to relativistic stabilization of the 7s-shell, the electron configuration of Cn^+ is different [13]. It actually is $[Rn]5f^{14}6d^{9}7s^2$. The electron is removed from the d-shell, instead of from the s-shell. This would mean that due to relativistic effects, the s-shell electron is bound stronger than the d-shell electron. This in turn means that the first IP obtained when removing the electron from the s-shell is larger than when removing it from the d-shell. We calculated the IPs for both cases. They are shown in table 1, where the character in brackets indicates from which shell the electron is removed. We indeed see that the IP is larger for the s-shell case, which confirms the prediction of the electronic configuration of Cn^+.

Comparing 2c, 4c and non-relativistic results

In table 2 the differences between two-component (2c), four-component (4c) and non-relativistic approach are shown. The non-relativistic approach is done with the four-component Hamiltonian and setting the value for the speed of light to 10000 in the input. The results are also shown in figure 3.

Table 2: First IPs in eV of Zn, Cd, Hg and Cn and their errors with respect to the experimental value in percents, within the CCSD(T) approach and using basis set dyall.v3z, comparing 2c, 4c and non-relativistic approach.

	Non-rel.	**Error**	**4c**	**Error**	**2c**	**Error**	***Experiment***
Zn	9,170	2,4	9,369	0,3	9,354	0,4	*9,394*
Cd	8,452	6,0	9,007	0,1	8,971	0,3	*8,994*
Hg	8,399	19,5	10,405	0,3	10,389	0,5	*10,438*
Cn	14,246(d)	-	11,811(d)	-	11,839(d)	-	11,969
	4,471(s)		13,556(s)		13,488(s)		11,779

The 4c and 2c approach give approximately the same accuracy. For Cn, the 2c approach took forty

minutes, while the 4c approach took two and a half hour. So, when time and computational resources are an issue, the 2c approach is a better option.

The non-relativistic results have a large error and we can see that relativistic effects play a larger role for heavier atoms, as expected.

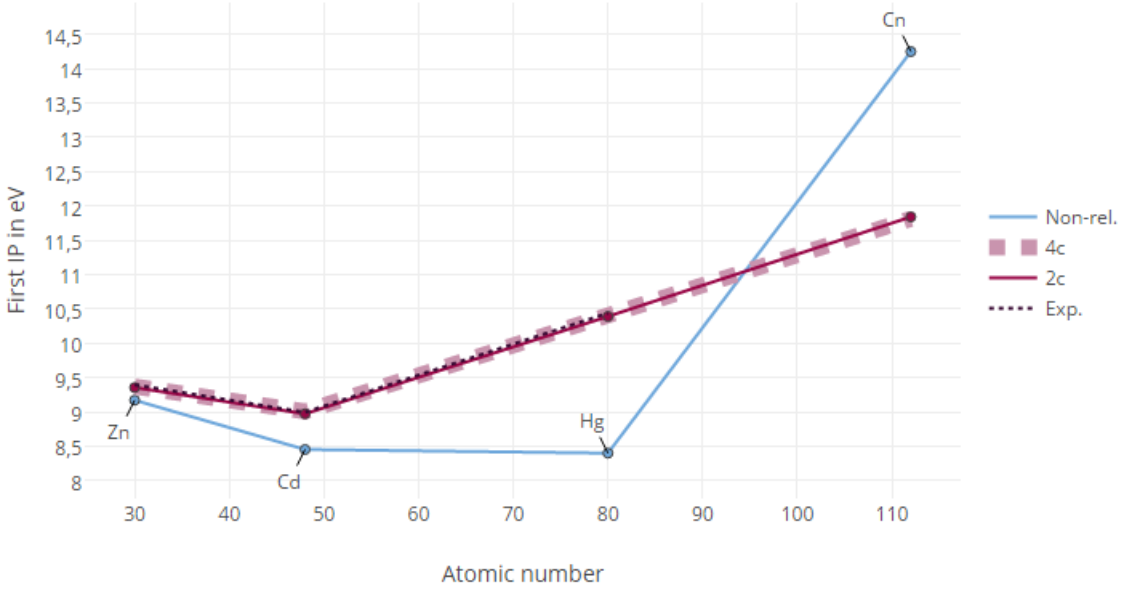

Figure 3: First IPs of group 12 elements

For all the cases in which an electron was removed from the s-shell, we see that the IP is lower than in the relativistic case. This can be explained by the fact that in the non-relativistic case, the s-shell electron doesn't experience the relativistic stabilization, hence is less bounded. For the other value of Cn, we see that the IP is actually higher than the relativistic one. This is because in the non-relativistic case the d-shell from where the electron is removed doesn't experience the relativistic destabilization, hence is stronger bound. Therefore, more energy is needed to remove the electron and the IP is higher in the non-relativistic case.

Comparing different basis sets

In table 3 the differences between different basis sets are shown. One can see that the larger the basis set, the smaller the error. The quadruple-zeta basis set gives the most accurate result. Even though the error is already small for the quadruple-zeta basis set, the difference between the quadruple- and triple-zeta results of Zn is still around 50 meV. This suggests that the calculations aren't fully converged yet, so using an even larger basis set could give even more accurate results.

Table 3: First IPs in eV of Zn, Cd, Hg and Cn and their errors with respect to the experimental value in percents, within 2c and CCSD(T) method, comparing different basis sets.

	dyall.v2z	**Error**	**dyall.v3z**	**Error**	**dyall.v4z**	**Error**	***Experiment***
Zn	9,181	2,3	9,354	0,4	9,407	0,1	*9,394*
Cd	8,849	1,6	9,007	0,1	8,995	0,0	*8,994*
Hg	10,256	1,7	10,405	0,3	10,439	0,0	*10,438*
Cn	11,764	-	11,839	-	11,481	-	11,969 11,779

For heavier atoms, the run time increases significantly for the larger basis sets though. For example, when the double-zeta basis set was used it took around eight minutes for Cn, while it took around two hours when the quadruple-zeta basis set was used.

3.1.2 Ionization potentials of group 1 elements[1]

In table 4 the calculated first and second IPs and non-relativistic IPs of lithium (Li), sodium (Na), potassium (K), rubidium (Rb), cesium (Cs), francium (Fr) and ununennium (Uue) are shown. Also the experimental values are included (cursive), or other theoretical values in the case an experimental value isn't available. The IPs are calculated using the two-component CCSD(T) approach and using the quadruple-zeta Dyall (dyall.v4z) basis set. For ununennium we couldn't use the Dyall basis set, since it isn't available yet for elements above Z=118. Therefore, the basis set of Faegri is used, obtained by adjusting the basis set of element 118 to heavier atoms [16].

Table 4: Relativistic and non-relativistic first and second IPs in eV of Li, Na, K, Rb, Cs, Fr and Uue and their errors with respect to the experimental value (exp.) in percents, within 2c and CCSD(T) method and using dyall.v4z.

	IP_1	**Error**	**IP_1 non-rel.**	**Error**	***IP_1 exp.***	**IP_2**	**Error**	**IP_2 non-rel.**	**Error**	***IP_2 exp.***
Li	5,389	0,1	5,389	0,1	*5,392* [15]	75,534	0,1	75,530	0,1	*75,64* [15]
Na	5,136	0,1	5,129	0,2	*5,139* [15]	47,027	0,5	47,119	0,4	*47,286* [15]
K	4,334	0,1	4,316	0,6	*4,340* [15]	31,494	0,4	31,597	0,1	*31,63* [15]
Rb	4,164	0,3	4,095	2,0	*4,177* [15]	27,157	0,5	27,429	0,5	*27,29* [15]
Cs	3,872	0,5	3,726	4,3	*3,893* [15]	23,029	0,6	23,481	1,4	*23,157* [15]
Fr	4,052	0,5	3,582	12,1	*4,073* [15]	20,673	-	21,765	-	20,02 [17]
Uue	4,783	-	3,383	-	4,793 [18]	12,847	-	19,958	-	20,3-21,4 [19]

We compare the second IP of Fr to the one obtained from calculations based on a simple spherical shell solution for neutral atoms [17]. The first IP of Uue is compared to the one obtained in CCSD calculations with the Dirac–Coulomb–Breit Hamiltonian [18]. The second IP of Uue is compared to a prediction made by investigating the trends in chemical groups [19].

We can again see that the heavier the atom, the more relativity plays a role. The electronic configuration of group 1 elements ends with an open s-shell. In non-relativistic calculations, we know

[1]The calculations in this subsection are done together with Koen van der Schoor.

that the relativistic energy stabilization of this shell isn't taken into account. This explains why the non-relativistic first IPs are smaller than the relativistic ones: it requires less energy to remove the valence electron.

The results are also shown in figure 5 and 6. One thing we see in figure 5 is that the relativistic trend goes up after it goes down. For the non-relativistic trend it only goes down. In heavier elements, the valence electron is further away from the nucleus. It is less attracted to the nucleus and therefore it is less bounded. This is an explanation for why the IP drops when the atomic number gets larger. Due to relativistic effects, the valence orbitals of the group 1 elements are contracted. This causes the valence electron to be closer to the nucleus, which is why the IP goes up again when the atomic number gets even larger. In the non-relativistic case, there is no contraction and the IP only drops.

We also see that in the case of the second IP, the non-relativistic values are larger than the relativistic values. To understand why this is, lets consider the electronic configuration of one of the group 1 elements. For neutral francium, it is $[Hg]6p^6 7s$ [15]. When this atom is doubly ionized, the 7s electron is removed and after that an electron from the 6p-shell is removed. When relativity is neglected, all the electrons in the p-shell have the same energy. In the relativistic case, electrons with orbital angular momentum larger than zero experience the spin-orbit splitting, which is the case for p-shell electrons. The energy level is divided according to the total angular momentum j (orbital angular momentum plus spin). For s-shell electrons (with zero orbital momentum) this means no splitting. For p-shell electrons (with orbital momentum of one) this means that the energy level is split in two (figure 4), one for total angular momentum $\frac{2}{3}$ and one for total angular momentum $\frac{1}{2}$.

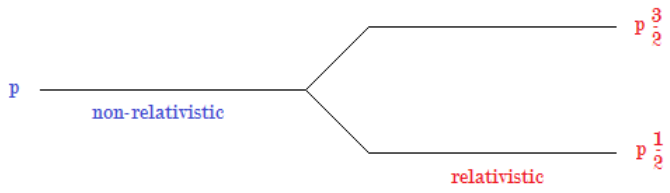

Figure 4: Schematic representation of the spin-orbit splitting of the p-shell.

The $p\frac{1}{2}$-orbitals and the s-orbitals are influenced most by direct relativistic effects, they are contracted and energetically stabilized. However, the $p\frac{3}{2}$-orbitals are significantly screened from the nucleus by the $p\frac{1}{2}$- and s-orbitals, causing destabilization of the $p\frac{3}{2}$-orbital. This indirect relativistic effect cancels most of the direct relativistic effect [20]. So, the $p\frac{3}{2}$-orbital lies higher in energy than the p-orbital would have been when relativistic effects were neglected. Therefore, the second IP is larger in the non-relativistic case. This effect is especially pronounced in element 119, because spin-orbit splitting becomes more pronounced when atomic number goes up.

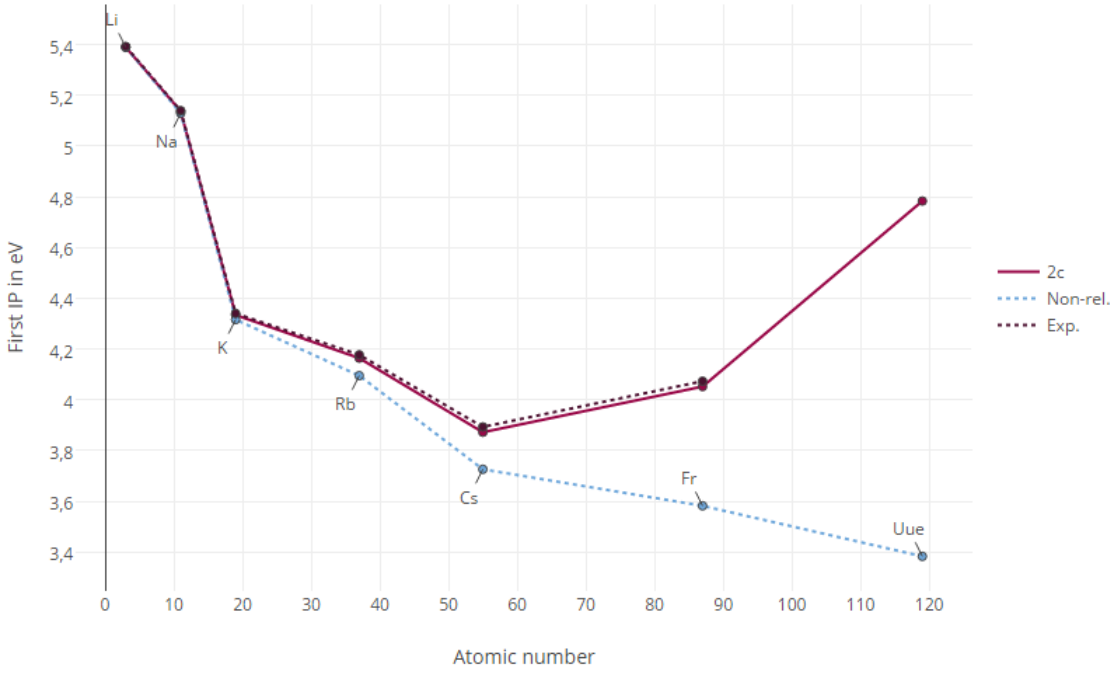

Figure 5: First IPs of group 1 elements

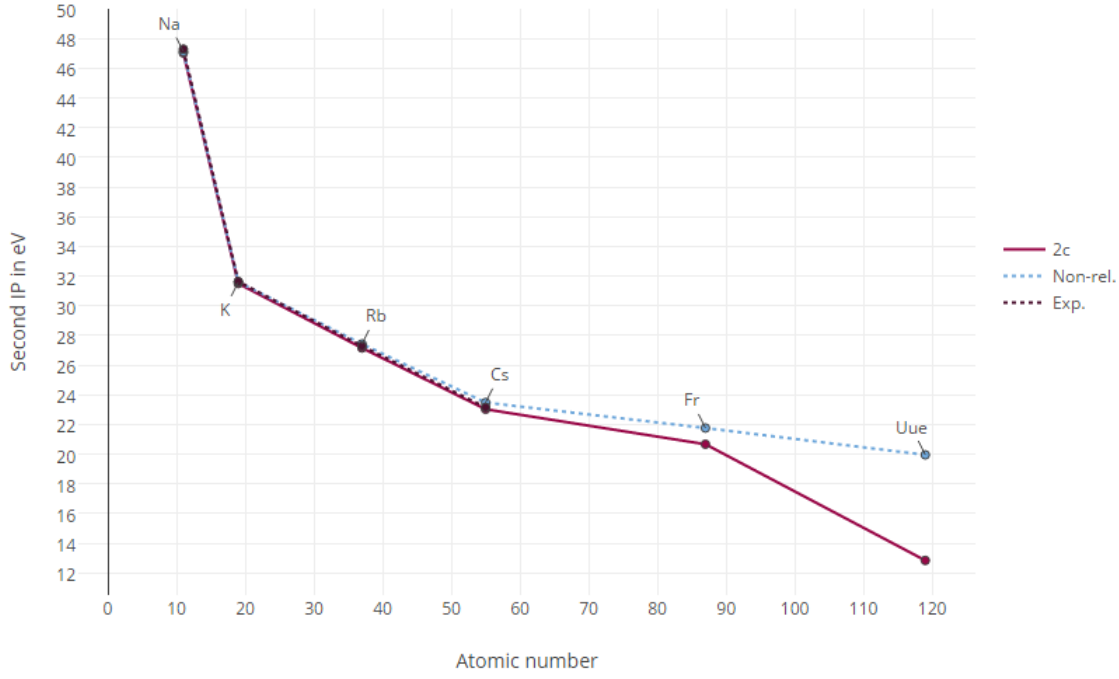

Figure 6: Second IPs of group 1 elements

3.2 Ionization potentials of einsteinium and holmium

Accurate experimental values of the first IP of einsteinium and holmium have been obtained (cursive in tables). The IPs have also been theoretically determined, using different methods. These previous results for holmium and einsteinium are listed in table 5 and 6, together with the results obtained in our calculations (bold in tables) using the four-component relativistic CCSD(T) method (R-CCSD(T) in table). Also the non-relativistic value (NR-CCSD(T) in table) is shown, obtained by setting the speed of light to 10000 Hartree in the input. For einsteinium the quadruple-zeta Dyall basis set was used and for holmium the triple-zeta Dyall basis set. The inner orbitals were 'frozen': the calculation of these orbitals were left out, without loss of accuracy in the results. Orbitals with energy less than -60 and -30 Hartree were omitted for respectively holmium and einsteinium. This was done to shorten the run time of the calculations.

Table 5: IPs in eV of einsteinium and their errors with respect to the experimental value in percents, calculated using various methods.

IP_1	**Error**	**IP_2**	**Method**	**Ref.**
6,07	4,7	12,20	PP+CASSCF+ACPF+SO[a]	[21]
6,04	5,1	12,19	PP+AEMCDHF+DC[b]	[21]
5,89	7,5	11,22	NN[c]	[22]
6,33	0,6	12,57	DFT+LDASIC+B[d]	[23]
5,742	9,8	-	DFT+LDA[e]	[24]
5,267	17,3	-	MCRDF[f]	[25]
6,380	**0,2**	**12,487**	**R-CCSD(T)**	-
5,331	**16,3**	**10,340**	**NR-CCSD(T)**	-
6,367	-	-	*RIMS*[g]	[26]

[a] relativistic ab initio pseudopotential (PP), complete active space self-consistent field (CASSCF), multi-reference averaged coupled-pair functional level (ACPF), corrected for spin-orbit (SO) effects, combined with extrapolations of the correlation contributions to the basis set limit.
[b] all-electron multi-configuration self-consistent field (AEMCDHF), Dirac-Coulomb Hamiltonian (DC), taking into account the errors of the applied pseudopotentials (PP).
[c] three-layer back-propagation neural network prediction.
[d] relativistic density functional all-electron calculations (DFT), local-density approximation with a self-interaction correction (LDASIC), Becke gradient exchange correction (B).
[e] density functional theory calculations (DFT), local density approximation (LDA) with Dirac exchange and neglecting Coulomb correlation.
[f] multiconfiguration relativistic Dirac-Fock.
[g] resonance ionization mass spectrometry.

Table 6: IPs in eV of holmium and their errors with respect to the experimental value in percents, calculated using various methods.

IP_1	Error	IP_2	Method	Ref.
5,83	3,2	11,62	PP+CASSCF+ACPF+SO[h]	[21]
4,621	23,3	8,487	HF[i]	[27]
6,680	10,9	-	MCHF[j]	[28]
6,022	-	11,80	SE[k]	[29]
6,013	**0,1**	**11,800**	**R-CCSD(T)**	-
6,778	**12,6**	**9,830**	**NR-CCSD(T)**	-
6,021	-	-	*MTDS*[l]	[30]

[h] relativistic ab initio pseudopotential (PP), complete active space self-consistent field (CASSCF), multi-reference averaged coupled-pair functional level (ACPF), corrected for spin-orbit (SO) effects, with contracted standard basis sets.
[i] Hartree-Fock method.
[j] multi-configuration Hartree-Fock, using non-relativistic Hamiltonian with relativistic corrections.
[k] semi-empirical extrapolation.
[l] magneto-optical trap depletion spectroscopy.

We can see that the first IP errors of the relativistic CCSD(T) are by far the smallest. These are 0,2% (0,013 eV) for einsteinium and 0,1% (0,006 eV) for holmium. The same accuracy is expected for the second IPs. The second IP of einsteinium is close to the value obtained using relativistic density functional all-electron calculations [23]. The second IP of holmium agrees with the value obtained using semi-empirical extrapolation [29].

The ground state electron configurations of neutral, ionized and doubly ionized einsteinium are respectively $[Rn]5f^{11}7s^2$, $[Rn]5f^{11}7s$ and $[Rn]5f^{11}$ [15]. When ionizing neutral einsteinium, an electron is removed from the s-shell. In non-relativistic calculations, the relativistic stabilization of the 7s-shell isn't taken into account and therefore the non-relativistic value for the first IP of einsteinium is lower than the relativistic one. The same can be said about the values for the second IP.

For holmium, the electron configuration for neutral, ionized and doubly ionized holmium are respectively $[Xe]4f^{11}6s^2$, $[Xe]4f^{11}6s$ and $[Xe]4f^{11}$ [15]. You would expect the the non-relativistic results to be both lower. This is the case for the second IP, but for the first IP it's actually higher. We couldn't find an explanation for this.

4 Conclusion

We have calculated the first IPs of group 12 elements using different methods and basis sets. The error in the results were significantly larger when using the DHF and CCSD method. From this we could conclude that electron correlation is important to include in order to get accurate results, where including single, double and pertubative triple excitations gave the best results.

Using a four component Hamiltonian and using the largest possible basis set gave the most accurate results, but the run time and the computational resources of the calculations also became significantly larger. When this is an issue, the two-component approach is a very good alternative to the four-component approach.

We have also calculated the relativistic and non-relativistic first and second IPs of group 1 elements. In the non-relativistic results we saw a large error, which could be explained by the fact that in these

calculations the relativistic energy stabilization or destabilization of the valence-shells was neglected. This error became larger with larger atomic number. From this we could conclude that relativity could not be neglected, especially not for heavy atoms. We also saw that not only the error of non-relativistic results was large, but that the non-relativistic results also failed to predict the correct trend in the IP. For group 1 elements, the non-relativistic calculations predicted a decrease in IP with increase of atomic number, while in reality there is a decrease and then an increase in IP.

With all this information we calculated the first and second IPs of holmium and einsteinium using the relativistic CCSD(T) method with the four-component Dirac-Coulomb Hamiltonian, using the quadruple-zeta Dyall basis set. We got values for the first IPs close to the experimental values with discrepancies of only milli-electronvolts. The second IPs of einsteinium and holmium have never been experimentally measured before. Here, we have made high quality predictions for the second IPs, where we expect the same accuracy as for the first IPs. From our results we can say that our approach has given the most accurate results thus far, and we provided reliable predictions where experiment is not yet available.

References

[1] A. Ghiorso. Einsteinium and fermium. *Chem. Eng. News*, **81**:174–175, 2003.

[2] H. G. Haire. *The Chemistry of the Actinide and Transactinide Elements*. The Netherlands. Springer, 2006.

[3] C. David Sherrill. http://vergil.chemistry.gatech.edu/notes/hf-intro/hf-intro.pdf, 2016.

[4] R. F. Bishop. The Coupled-Cluster Method. *Phys. Tod.*, **40**:52–60, 1987.

[5] V. Pershina. *Theoretical Chemistry of the Heaviest Elements*. Berlin. Springer, 2003.

[6] P. Pyykkö. Relativistic Effects in Structural Chemistry. *Chem. Rev.*, **88**:563–594, 1988.

[7] U. Kaldor. Quantum Chemistry (Heavy Atoms and Molecules). Tel Aviv University.

[8] T. Saue. Relativistic hamiltonians for chemistry: a primer. *Chem. Phys. Chem.*, **12**:3077–3094, 2011.

[9] A. Borschevsky. http://www.tau.ac.il/∼ ephraim/Appendix_1.pdf, 2016.

[10] R. Bast, T. Saue, L. Visscher and H. J. Aa. Jensen. http://www.diracprogram.org, 2016.

[11] M. Barysz. *Relativistic Methods for Chemists*. New York. Springer, 2010.

[12] Dyall basis sets. http://dirac.chem.sdu.dk/basisarchives/dyall/index.html, 2016.

[13] E. Eliav and U. Kaldor. Transition energies of mercury and ekamercury (element 112) by the relativistic coupled-cluster method. *Phys. Rev. A*, **52**:2765–2769, 1995.

[14] K. G. Dyall. Relativistic double-zeta, triple-zeta, and quadruple-zeta basis sets for the 6d elements Rf–Cn. *Theor. Chem. Acc.*, **129**:603–613, 2011.

[15] NIST. http://physics.nist.gov/physrefdata/handbook/periodictable.htm, 2016.

[16] K. Faegri. Relativistic Gaussian basis sets for the elements K – Uuo. *Theor. Chem. Acc.*, **105**:252–258, 2001.

[17] T. A. Carlson. Calculated ionization potentials for multiply charged ions. *At. Data Nucl. Data Tables*, **2**:63–99, 1970.

[18] E. Eliav et al. Ionization potentials of alkali atoms: towards meV accuracy. *Chem. Phys.*, **311**:163–168, 2005.

[19] D. Bonchev and V. Kamenska. Predicting the Properties of the 11 3-120 Transactinide Elements. *J. Phys. Chem.*, **85**:1177–1186, 1981.

[20] K. G. Dyall and K. Faegri. *Introduction to relativistic quantum mechanics.* New York. Oxford University Press, 2007.

[21] X. Cao and M. Dolg. Theoretical prediction of the second to fourth actinide ionization potentials. *Mol. Phys.*, **101**:961–969, 2003.

[22] M. E. Sigman and S.S. Rives. Prediction of Atomic Ionization Potentials 1-111 Using an Artificial Neural Network. *J. Chem. Inf. Comput. Sci*, **34**:617–620, 1994.

[23] W. Liu, W. Küchle and M. Dolg. Ab initio pseudopotential and density-functional all-electron study of ionization and excitation energies of actinide atoms. *Phys. Rev. A*, **58**:1103–1110, 1998.

[24] N. A. Cordero, N. H. March and J. A. Alonso. Ionization potentials of neutral atoms and positive ions in the limit of large atomic number. *Phys. Rev. A*, **75**:012505.1–012505.8, 2007.

[25] M. Cory et al. An intermediate neglect of differential overlap technique for actinide compounds. *J. Phys. Chem.*, **100**:1353–1365, 1994.

[26] N. Erdmann et al. Determination of the first ionization potential of nine actinide elements by resonance ionization mass spectroscopy (RIMS). *J. Alloy. Compd.*, **271-273**:837–840, 1998.

[27] P.R. Librelon and F.E. Jorge. Gaussian Basis Sets for the Calculation of Some States of the Lanthanides. *Braz. J. Phys.*, **21**:322–326, 2001.

[28] G. Gaigalas, Z. Rudzikas and T. Žalandauskas. Studies of Lanthanides 6s Ionization Energy. *Lith. J. Phys.*, **44**:249–257, 2004.

[29] W. C. Martin, R. Zalubas and L. Hagan. *Atomic Energy Levels - The Rare Earth Elements.* Washington. U.S. Dept. of Commerce, National Bureau of Standards, 1987.

[30] J. Hostetter et al. Measurement of holmium Rydberg series through magneto-optical trap depletion spectroscopy. *Phys. Rev. A*, **91**:012507.1–012507.7, 2015.